Journal of Molecular Liquids 379 (2023) 121680

Contents lists available at ScienceDirect

Journal of Molecular Liquids

journal homepage: www.elsevier.com/locate/molliq

Molecular dynamics study on the kinematic viscosity, density and structure of fuel blends containing n-decane and biofuel compound of ethyl decanoate or ethyl dodecanoate

Xueming Yang [a,*], Qiang Liu [a], Yongfu Ma [a], Jianfei Xie [b], Bingyang Cao [c,*]

[a] Hebei Key Laboratory of Low Carbon and High Efficiency Power Generation Technology, Department of Power Engineering, North China Electric Power University, Baoding 071003, China

[b] School of Computing and Engineering, University of Derby, Derby DE22 3AW, United Kingdom

[c] Key Laboratory for Thermal Science and Power Engineering of Ministry of Education, Department of Engineering Mechanics, Tsinghua University, Beijing 100084, China

ARTICLE INFO

Article history:
Received 6 January 2023
Revised 23 February 2023
Accepted 18 March 2023
Available online 21 March 2023

Keywords:
Thermophysical properties
Molecular dynamics
Molecular structures
Fuel blend

ABSTRACT

Bio-aviation fuel is blend consisting of aviation kerosene and biofuels, which is a clean renewable energy and has gained considerable attention in recent years. However, numerical studies on the thermophysical properties of bio-aviation fuel containing fatty acid esters are still limited. In this paper, the kinematic viscosity and density of fuel blends containing n-decane and biofuel compound of ethyl decanoate or ethyl dodecanoate are investigated by molecular dynamics (MD) method, and the calculated viscosities are compared with those by a theoretical model of UNIFAC-VISCO (UV). The MD results applying with a PCFF force field (FF) can reproduce the experimental data for the fuel blends very well in comparison with both the COMPASS FF and the UV model. In addition, to link the variety of molecular structure to the changes of their thermophysical properties, local structures of n-decane and ethyl decanoate in mixture are systematically analyzed. It illustrates that a decreasing end-to-end length of molecular chains combined with the growing intermolecular distance leads to the reduction of the kinematic viscosity of fuel blends with the increasing of temperature. This work provides a baseline to help understand the thermophysical properties of esters and their based bio-aviation kerosene surrogates.

© 2023 Elsevier B.V. All rights reserved.

1. Introduction

Primary pollution caused by the harmful gases and fine particles emitted from the fossil aviation fuel combustion has attracted lots of attention [1,2]. Interests on new clean aviation fuel and its additives have been becoming an indispensable and imperative commission. Bio-aviation kerosene prepared by adding biofuel to fossil aviation fuels has also been tested on the aircraft, proving that bio-aviation kerosene can provide stable and reliable power for the aircraft and significantly reduce the emission of hazardous gases such as CO and NOx generated during combustion [3]. In addition, the development of bio-aviation kerosene has become a vital step to cope with the shortage of fossil energy.

The composition of real jet fuels is highly complicated and contains a large number of components, which makes it difficult to study their thermophysical properties and combustion characteristics. To solve this problem, surrogates composed of one or several simple components [4,5] had been suggested to capture either thermophysical or combustion characteristics of complex fluids such as jet fuels to simplify the calculations. Among them, fuel surrogates based on alkanes have been extensively studied. Since N-decane can well characterize the content of alkanes in aviation fuel by virtue of both its moderate molecular weight and low ratio of hydrogen to carbon, it is usually used to replace aviation fuels, i.e., Jet Propellant-8 (JP-8) [6,7] and Rocket Propellant-3 (RP-3) [8]. Liu *et al.* [9] studied the distributions of soot particle size for RP-3 on the stable flame retarding platform of the burner by using one-component surrogate (n-decane) and two-component surrogate (n-decane/1,2,4 – trimethylbenzene). Zhao *et al.* [7] utilized a high temperature chemical reactor to study the pyrolysis process of n-decane, which was taken as a single-component surrogate of aviation kerosene JP-8 at 1100–1600 K and 600 Torr pressure. Most of the present work studying the thermophysical properties of biofuels or their surrogates were mainly focused on the experiment investigations but rarely focused on the theory or simulations. There are two typical biofuel compounds, i.e., ethyl decanoate

* Corresponding authors.
E-mail addresses: xuemingyang@ncepu.edu.cn (X. Yang), caoby@tsinghua.edu.cn (B. Cao).

https://doi.org/10.1016/j.molliq.2023.121680
0167-7322/© 2023 Elsevier B.V. All rights reserved.

and ethyl dodecanoate. Zhang *et al.* [10] measured the speed of sound and thermal diffusivity of ethyl decanoate in a large range of temperatures and pressures. He *et al.* [11] measured the density and viscosity for both methyl dodecanoate and ethyl dodecanoate at temperatures ranging from 302 K to 354 K. Zhao *et al.* [12] employed the surface light scattering (SLS) approach to simultaneously measure the liquid surface tension and kinematic viscosity of different binary mixtures of n-hexadecane, methyl butyrate and methyl decanoate at temperatures ranging from 353.15 K to 423.15 K. The liquid density of the binary mixtures at temperatures of 293.15–423.15 K were obtained by a U-tube densitometer.

Molecular dynamics (MD) simulation, which has capacity of assessing the molecular level information, is a powerful tool to investigate the thermophysical properties of fluids [13–16]. In recent years, MD has been widely used to study the thermophysical properties of complex fluids such as fuels [17–19] and liquid organic mixtures [20,21]. Wang *et al.* [17] performed equilibrium molecular dynamics (EMD) simulations to predict the sub-to-supercritical properties (i.e., the shear viscosity, the bulk density, and the thermal conductivity) of the jet fuel JP-10 with three different force fields (FFs): two all-atom FFs (COMPASS (II), OPLS-AA), and one united-atom FF (TraPPE-UA). The two all-atom FFs can produce the thermophysical properties in both gas and liquid phases, while large divergences are reported in the transition and critical regions. Yang *et al.* [18,19] used EMD to investigate the thermal conductivities, densities and viscosities of surrogate fuel (mixture of 1,2,4-trimethylbenzene/n-decane) and Rocket Propellant (RP-3), with COMPASS and of TraPPE-UA force fields, respectively. Their EMD results were in good agreement with the data from NIST SUPERTRAPP [22]: for viscosities, AARD (average absolute relative deviation) generated by the COMPASS FF was 4.44%; and for thermal conductivities, AARD generated by the TraPPE-UA FF was 3.417%. Maskey *et al.* [20] investigated the hydrocarbon mixtures and pure components of n-alkylcyclohexanes, n-alkylbenzenes, and n-alkanes using MD simulations. All simulations reproduced most of the thermophysical properties including density, bulk modulus, and the excess molar volume as a function of n-alkylbenzene side-chain length, n-alkane length, and composition. Luning *et al.* [21] investigated some thermophysical properties (i.e., density and excess molar volume) of two binary mixtures of n-dodecane with either n-dodecylcyclohexane or n-propylcyclohexane at the temperature range of 293.15 – 333.15 K.

However, the MD studies of thermophysical properties of a bio-aviation fuel containing fatty acid esters are still limited. Yuan *et al.* [23] investigated the liquid kinematic viscosity and surface tension of the proposed biofuel surrogates of *iso*-octane with methyl hexanoate, n-decane with methyl decanoate, and methyl octanoate by MD simulation with GROMOS FF over temperatures ranging from 313.15 K to 423.15 K. Their results showed good comparability with both the experimental data and simulation results for the kinematic viscosity of a mixture of n-decane with methyl decanoate and a mixture of n-decane with methyl octanoate. However, big difference was reported for a mixture of *iso*-octane with methyl hexanoate, particularly at lower temperatures. As far as we are aware, there are no MD investigations into the viscosity and density of ethyl decanoate and ethyl dodecanoate or their mixtures consisting of one of the two components. In this paper, thermophysical properties of the fuel blends containing n-decane and biofuel compound of ethyl decanoate or ethyl dodecanoate are studied by EMD simulations. Both the COMPASS and the PCFF force fields are adopted to calculate the viscosity and density in the simulations, and we make a comparison of the viscosity results with those predicted by a theoretical model of UNIFAC-VISCO (UV). Detailed structural analysis are made to gain a better insight of the binary mixture's viscosity and density from the microscopic perspective. The numerical data is provided in supplementary information for readers to compare the MD simulation results.

2. Methodology

2.1. Force fields

In this study, we apply two all-atom FFs, i.e., the COMPASS FF and the PCFF FF. The functional form and the details of the PCFF FF and the COMPASS FF can be found in Ref. [24] and Ref. [25], respectively. Compared to the PCFF FF, the COMPASS FF shares a similar potential function form, but includes the additional cross-coupling terms: $E_{b,\varphi}$, $E_{\theta,\varphi}$, and $E_{\theta,\theta,\varphi}$[25], which are the bond-angle term, the angle-torsion term, and the angle-angle-torsion term, respectively. The bonded parameters for the COMPASS FF are taken from Ref. [25] and those for the PCFF FF are taken from Refs. [26,27].

Tables 1 and 2 list the definitions of different groups and the non-bonded parameters for the COMPASS FF and the PCFF FF, respectively. In Table 2, ε is the LJ energy parameter and σ is the LJ length parameter. In this study, the Sixth-order mixing rules are used to describe the interactions between the unlike atoms for MD simulations with the COMPASS FF, and the Lorentz-Berthelot (LB) mixing rules [28] are used for MD simulations with the PCFF FF. The expressions of the two mixing rules including the Sixth-order and the LB are shown in Eqs. (1) and (2), respectively. In fact, the Sixth-order mixing rules have been commonly used to produce the non-bonded parameters of the COMPASS FF for alkanes and fatty acid esters [29–31]. Importantly, our recent study [18] has found that, for the COMPASS FF, the Sixth-order mixing rules has a better numerical accuracy in prediction of viscosity and density than the LB mixing rules for some compounds such as the n-decane in alkane and the aromatic compound. Here we use LB mixing rules rather than the Sixth-order mixing rules for PCFF FF because our case study shows the non-bonded parameters generated by the Sixth-order mixing rules will lead to very big errors in simulating the density of the biofuel compound. The details of the case study will be provided in Section 3.

$$\varepsilon_{ij} = 2\sqrt{\varepsilon_i \varepsilon_j}\left(\frac{(\varepsilon_i)^3 \cdot (\varepsilon_j)^3}{(\varepsilon_i)^6 + (\varepsilon_j)^6}\right) \quad \text{Sixth-order mixing rules} \qquad (1)$$
$$\sigma_{ij} = \left(\frac{(\sigma_i)^6 + (\sigma_j)^6}{2}\right)^{1/6}$$

$$\varepsilon_{ij} = \sqrt{\varepsilon_i \varepsilon_j} \quad \text{LB mixing rules} \qquad (2)$$
$$\sigma_{ij} = \left(\frac{\sigma_i + \sigma_j}{2}\right)$$

2.2. Estimate of viscosity

The EMD method with Green-Kubo (GK) formula is employed to calculate the fluid viscosity. In fact, the predicted results by EMD or non-equilibrium molecular dynamics (NEMD) methods are generally comparable. For example, Kondratyuk *et al.* [32] carried out MD simulation on the viscosity of branched alkanes adopting the

Table 1
Definitions of different atom types.

Atom type	Definition
C_{H3}	Methyl group
C_{H2}	Secondary sp3 carbon in linear alkyl chains
C	Carbonyl carbon
OC	Ester oxygen
O	Carbonyl oxygen
H	Hydrogen

Table 2
The non-bonded parameters of the PCFF and COMPASS FFs [27].

	COMPASS		PCFF	
Atom type	ε (kJ /mol)	σ (Å)	ε (kJ /mol)	σ (Å)
C_{H3}	0.2594	3.854	0.2259	4.01
C_{H2}	0.2594	3.854	0.2259	4.01
C	0.2678	3.9	0.5021	3.81
OC	0.4017	3.3	1.0042	3.42
O	0.8033	3.43	1.1171	3.3
H	0.0962	2.878	0.0837	2.995

COMPASS II FF, and their results showed that the calculated viscosities with both NEMD and EMD methods were consistent at low pressures (i.e., 100 MPa). GK is used to calculate the shear viscosity and is given as follows:

$$\eta = \frac{V}{3k_BT}\int_0^\infty \sum_\alpha \sum_\beta \langle P_{\alpha\beta}(0)P_{\alpha\beta}(t)\rangle \mathrm{d}t \quad (3)$$

where V represents the system volume, k_B is the Boltzmann constant, T is the system temperature, α and β denote the x, y and z directions in Cartesian coordinates ($\alpha \neq \beta$), the angle bracket denotes the average of the autocorrelation function, and $P_{\alpha\beta}(t)$ represents the components of the pressure tensor in the α- and β-directions at time t. The kinematic viscosity v in this paper is obtained by dividing the shear viscosity by density.

2.3. Molecular dynamics simulation

The Large-scale Atomic/Molecular Massively Parallel Simulator (LAMMPS) [33], which is a commonly used Open-source code, is employed in all MD simulations. Each simulation is conducted in a 3D cubic box, and the periodic boundary conditions are applied to all the three directions, i.e., x-, y- and z. The length of the simulation cube is set to 60 Å×60 Å×60 Å initially. The Newton's equations for tracking the atom motions are integrated in terms of the velocity Verlet algorithm with a time step of 0.4 fs. The long-range electrostatic interactions are calculated using the particle–particle particle–mesh (PPPM) method, which uses a cutoff distance of 14 Å and an accuracy of 10^{-4} in force [34]. A cutoff distance of 14 Å is applied for LJ interactions. The applied cut-off distance is large enough ($> 3.5\sigma$, where σ is 3.854 Å for C_{H2}) and compatible with the literatures [19], allowing the simulations to keep a reasonable balance between accuracy and efficiency. A long-range tail correction is applied for van der Waals interactions larger than the cut-off radius. Initially, the simulations proceed with a NPT ensemble with the Nose-Hoover thermostat, under which both pressure and temperature are controlled, and the system is equilibrated at the given pressure and temperature for 1.5 ns; after that, the simulation is switched to a NVT ensemble with the Nose-Hoover thermostat, and the system is further relaxed at a given temperature for another 1 ns. The viscosity and density are calculated in the following 1 ns.

Six independent simulations have been performed in this work for both pure fluids and their mixtures and the initial velocity is modified to dismiss the uncertainties for each independent run in EMD simulations [35]. We assign the initial velocities randomly but their distribution obeys the Gaussian one. The unique initial velocity distributions are generated by a different seed number under the same conditions in each independent run. Both the mean viscosity and density are evaluated under the given temperature and pressure by averaging over their values in each of the six independent runs.

There are 400 molecules in total in each simulation system. The total number of molecules in a pure ethyl decanoate or ethyl dodecanoate system is 400, equivalent to 15,200 or 17,600 atoms in total. Experimental data of kinematic viscosity and density of pure ethyl decanoate or ethyl dodecanoate are from literature [11,36]. For the n-decane/ethyl decanoate or ethyl dodecanoate mixture, 300n-decane molecules and 100 ethyl decanoate or ethyl dodecanoate molecules are employed as shown in Fig. 1, which is corresponding to the n-decane/ethyl decanoate mixture (mole fraction of 75% n-decane and 25% ethyl decanoate) and the n-decane/ethyl dodecanoate mixture (mole fraction of 75% n-decane and 25% ethyl dodecanoate) experimentally studied by Yuan *et al.* [37].

2.4. Theoretical prediction

To calculate the viscosities for the mixtures theoretically, the UV model [38,39] is adopted and is given by

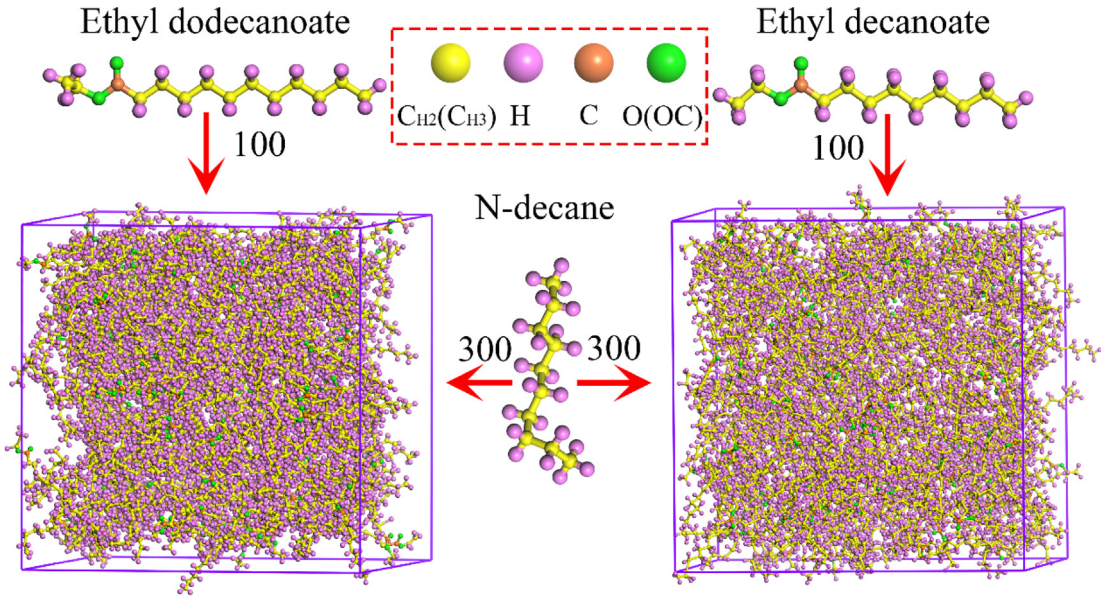

Fig. 1. Schematic of a simulation system for mixtures with a total molecular number N = 400.

Table 3
Group volume and surface area parameters in the UV model.

Group k	R_k	Q_k
C_{H2}	0.6744	0.540
C_{H3}	0.9011	0.848
COO	1.0020	0.880

Table 4
Group interaction parameters α_{nm} in the UV model.

n/m	C_{H2}	C_{H3}	COO
C_{H2}	0	66.53	1172.0
C_{H3}	−709.5	0	−172.4
COO	541.6	−44.25	0

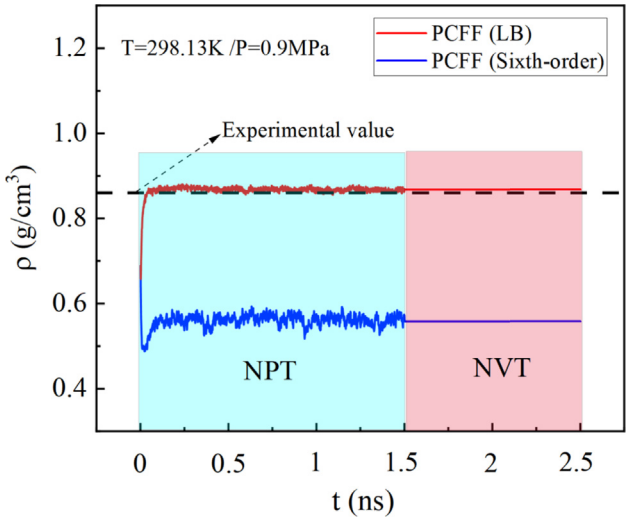

Fig. 2. Comparison of simulated density by PCFF FF with two different mixing rules: the LB and the Sixth-order.

$$\ln(v_m\rho_m) = \sum_i x_i \ln(v_i\rho_i V_i) - \ln V_m + \frac{\Delta * g^{EC}}{RT} + \frac{\Delta * g^{ER}}{RT} \tag{4}$$

where v_m, ρ_m, and V_m are the kinematic viscosity, density, and molar volume of the mixture, respectively; x_i, v_i, and V_i are the mole fraction, the kinematic viscosity, and the molar volume of pure component i, respectively. $\Delta * g^{EC}/RT$, $\Delta * g^{ER}/RT$ are the mixed terms, and $\Delta * g^{EC}/RT$ can be calculated as follows:

$$\frac{\Delta * g^{EC}}{RT} = \sum_i x_i \ln\left(\frac{\phi_i}{x_i}\right) + \left(\frac{z}{2}\right)\sum_i q_i x_i \ln\left(\frac{\theta_i}{\phi_i}\right) \tag{5}$$

where ϕ_i and θ_i are the molecular volume fraction and the molecular surface area fraction, which are given by Eqs. (6) and (7), respectively, and z is a constant having value of 10.

$$\phi_i = \frac{x_i r_i}{\sum_j x_j r_j} \tag{6}$$

$$\theta_i = \frac{x_i q_i}{\sum_j x_j q_j} \tag{7}$$

where r_i is the van der Waal's volume and q_i is the van der Waal's surface area of component i, which can be obtained by summing the corresponding group contributions. Their formulae are given as follows:

$$r_i = \sum_k n_k^{(i)} R_k \tag{8}$$

$$q_i = \sum_k n_k^{(i)} Q_k \tag{9}$$

where k is the group index, n_k^i is the number of k groups in molecule i, R_k and Q_k are respectively the volume parameter and surface area parameter of a group k, which are given in Table 3.

The mixed term $\Delta * g^{ER}/RT$ in Eq. (4) can be computed as follows:

$$\frac{\Delta * g^{ER}}{RT} = -\sum\left(x_i \cdot \sum_k n_k^i \left[\ln\gamma_k^* - \ln\gamma_k^{*(i)}\right]\right) \tag{10}$$

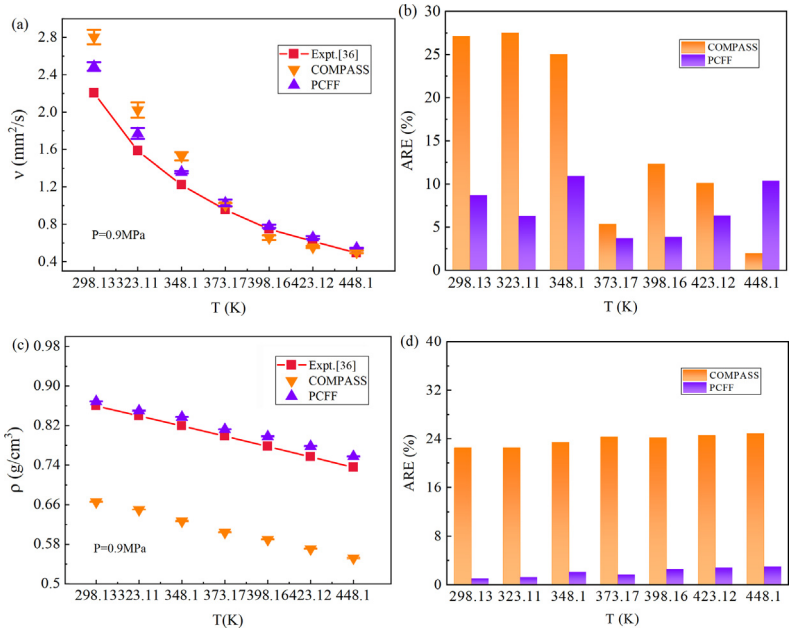

Fig. 3. Viscosity and density of pure ethyl decanoate vary with the increasing of temperature in EMD simulations with different FFs and corresponding AREs: (a) and (b) viscosity; (c) and (d) density.

where γ_k^* and $\gamma_k^{*(i)}$ are the coefficients of group k in a mixture of groups in the actual mixture and the pure component i, respectively. Parameters γ_k^* can be calculated below:

$$\ln \gamma_k^* = Q_k \left[1 - \ln \left(\sum_m \Theta_m \psi_{mk}^* \right) - \sum_m \frac{\Theta_m \psi_{km}^*}{\sum_n \Theta_n \psi_{nm}^*} \right] \tag{11}$$

where Θ_m and X_m are the surface area fraction and mole fraction in groups mixtures given in Eq. (12), ψ_{nm}^* is the interaction parameter shown in Eq. (13), and α_{nm} are group interaction parameters, whose values are listed in Table 4 and the subscript nm represents the interaction between group n and group m.

$$\Theta_m = \frac{Q_m X_m}{\sum_k X_k Q_k} \tag{12}$$

$$\psi_{nm}^* = \exp\left(-\frac{\alpha_{nm}}{298}\right) \tag{13}$$

3. Results and discussion

The viscosity and density of pure ethyl decanoate, pure ethyl dodecanoate, and their mixtures with n-decane are calculated. The calculated results are compared to the experimental data in terms of an absolute relative error (ARE):

$$ARE = \frac{\left| A^{CAL} - A^{Expt.} \right|}{A^{Expt.}} \times 100\% \tag{14}$$

where A^{CAL} are the values of viscosity or density obtained by either MD simulations or theoretical predictions, A^{Expt} denotes the values from the experiment, and the average AREs is simplified as AAREs.

To find out the right mixing rules representing the interactions between the unlike atoms in MD simulations with the PCFF FF, we perform a case study to make a comparison of density predictions between two mixing rules including both the LB and the Sixth-order for PCFF FF at 298.13 K and under 0.9 MPa, as shown in Fig. 2. It is found that the simulated density by the PCFF FF with the LB mixing rules agrees well with the experimental data with an error of only 1.17% but very large error is reported when using the Sixth-order mixing rules for PCFF FF. The error of density calculated by the Sixth-order mixing rules for PCFF FF is 34.8%, which is less than the experimental value. This may indicate that the Sixth-order mixing rules for PCFF FF lead to a strong repulsive not to

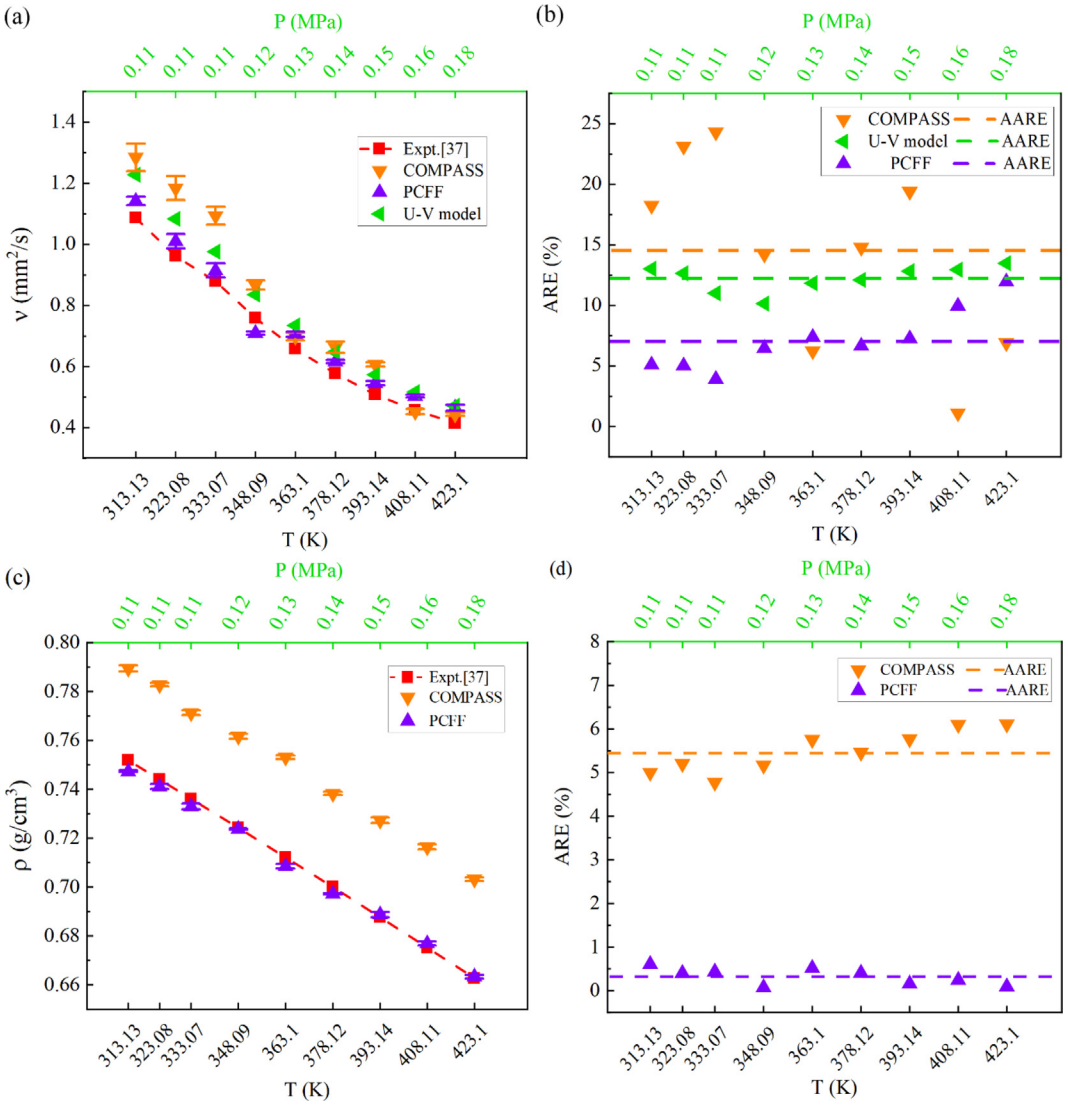

Fig. 4. Kinematic viscosity and density calculated by either EMD simulations or the UV model for n-decane/ethyl decanoate mixture and corresponding AREs: (a) and (b) viscosity; (c) and (d) density.

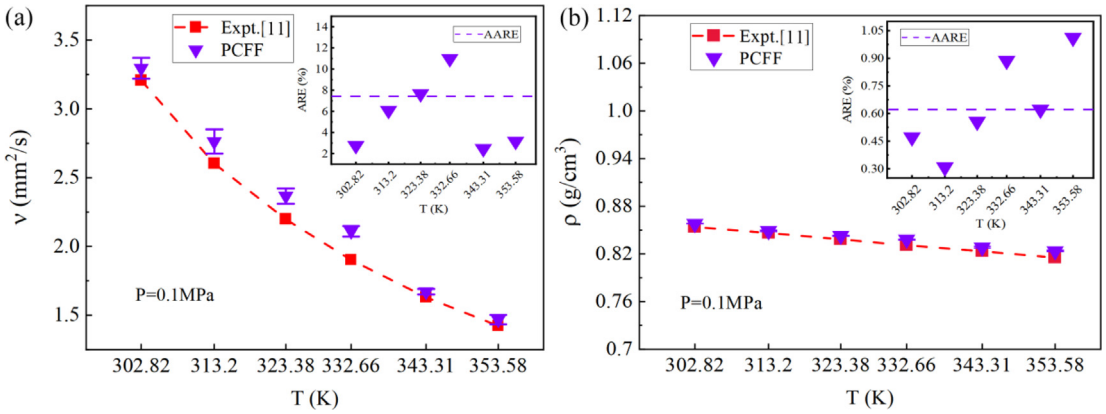

Fig. 5. Kinematic viscosity and density of pure ethyl dodecanoate calculated by EMD simulations and the corresponding AREs: (a) viscosity; and (b) density.

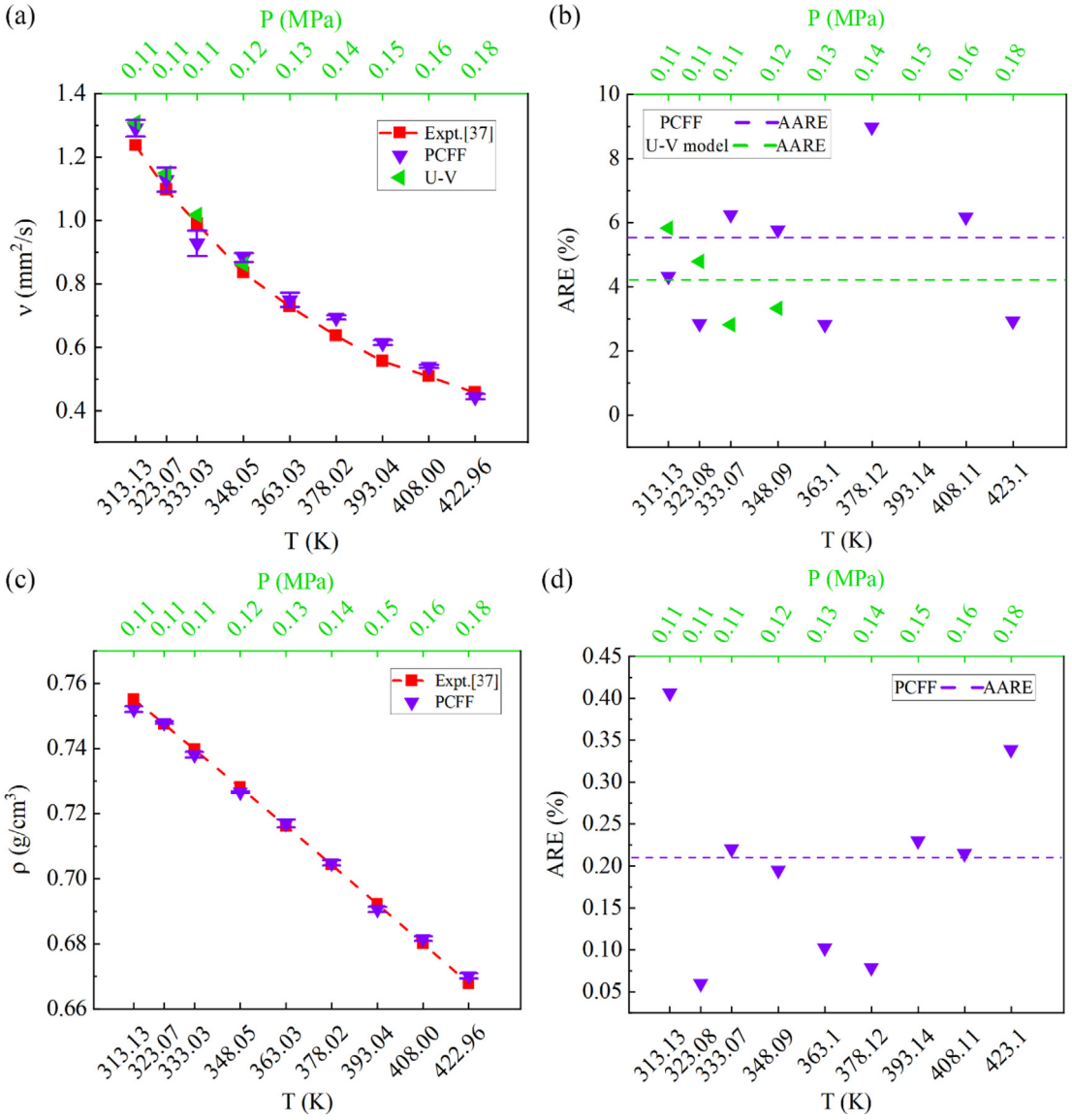

Fig. 6. Kinematic viscosity and density calculated by either EMD simulations or the UV model for n-decane/ethyl dodecanoate mixture and the corresponding AREs: (a) and (b) viscosity; (c) and (d) density.

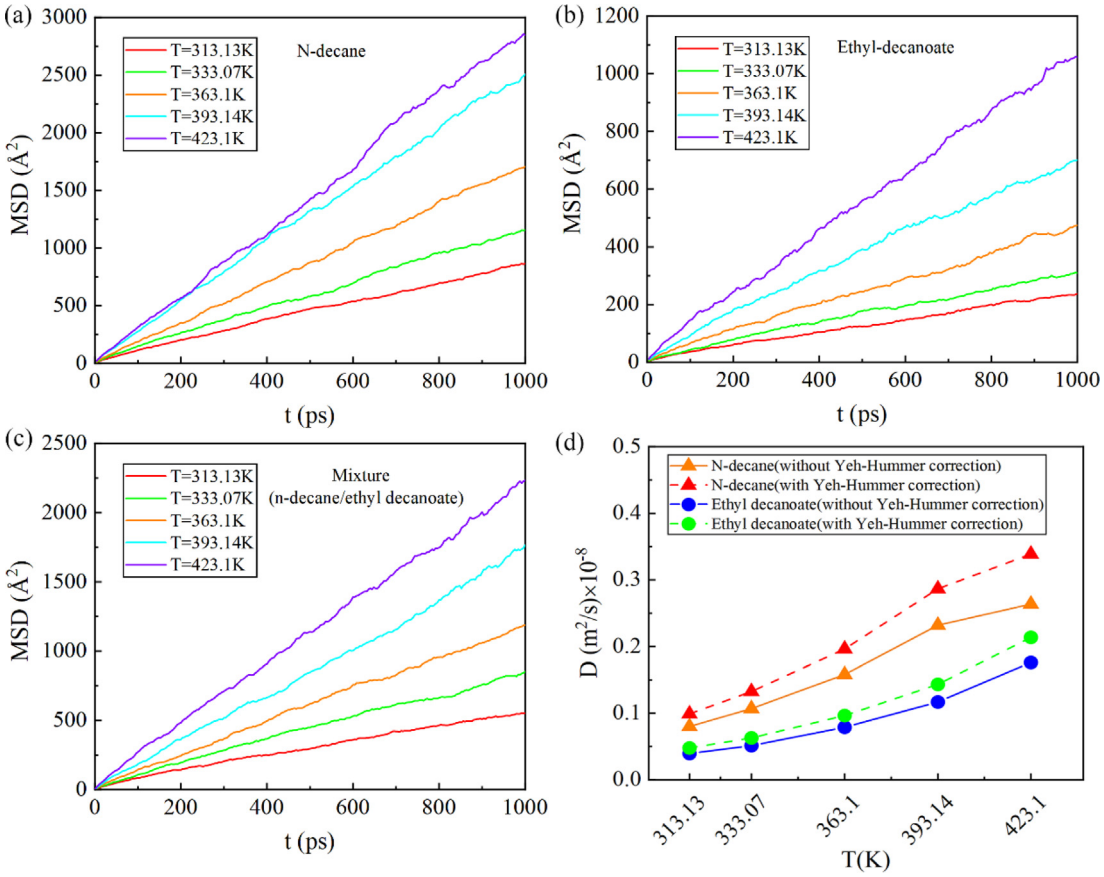

Fig. 7. Both MSDs (a) – (c) and (d) the self-diffusion coefficient D vary at different temperatures.

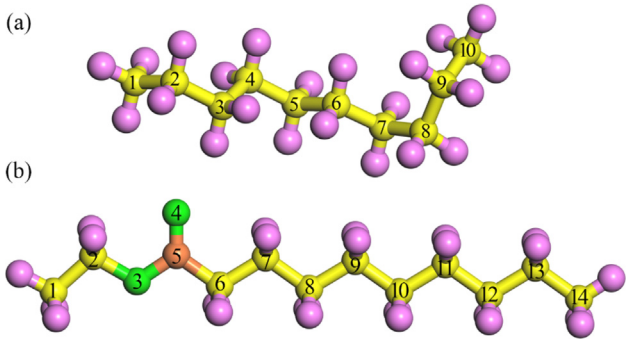

Fig. 8. Index of atoms: (a) n-decane; and (b) ethyl decanoate.

accurately represent ethyl decanoate interactions. Therefore, the LB mixing rules for the PCFF FF is used and recommended in the following simulations.

3.1. Viscosity and density of ethyl decanoate and its mixture with n-decane

Both the viscosity and density of pure ethyl decanoate and its binary mixture with alkane component n-decane are simulated in terms of two FFs, i.e., COMPASS and PCFF. There is a comparison of simulation results with the experimental data [37].

The simulation results of two FFs on the viscosity and density of ethyl decanoate and the corresponding AREs at temperatures from 298.13 K to 448.1 K under 0.9 MPa can be found in Fig. 3, in which the experimental data are also presented [36]. It indicates that both FFs mimic the decreasing trend of viscosity and density as temperature increases. The AAREs of the simulated viscosity and density by the PCFF FF are 9.11% and 2.08%, respectively, and those by the COMPASS FF are 15.64% and 23.8%. It shows that the PCFF FF outperforms the COMPASS FF in predicting the viscosity and density of ethyl decanoate.

Both viscosities and densities in MD simulations by the COMPASS FF and the PCFF FF for a binary mixture of n-decane and ethyl decanoate under different pressures at temperatures from 313.13 K to 423.1 K can be found in Fig. 4. The corresponding experimental data [37] and the calculated viscosities by the UV model are also included in Fig. 4. The variation trend of both viscosities and densities are consistent with the experimental data. The AAREs of the simulated viscosity and density by the PCFF FF are 7.08% and 0.32%, respectively, and those by the COMPASS FF are 14.26% and 5.48%. This also suggests that the PCFF FF has better prediction performance than the COMPASS FF in describing the viscosity and density of a binary mixture of n-decane and ethyl decanoate. The UV model has an AARE of 12.22% for calculating the viscosities of binary mixture of n-decane and ethyl decanoate, thus it is inferior to EMD method with the PCFF FF.

It should be noted that the prediction of thermophysical properties using MD simulations fairly depends on the adopted FF. Our previous work [18] has reported that the COMPASS FF with Sixth-order mixing rules can well predict the viscosity and density of n-decane, however, it exhibits relatively large deviations when simulating the density of pure ethyl decanoate and their mixtures with n-decane. This may suggest that the COMPASS FF with Sixth-order mixing rules is less accurate to predict the densities and vis-

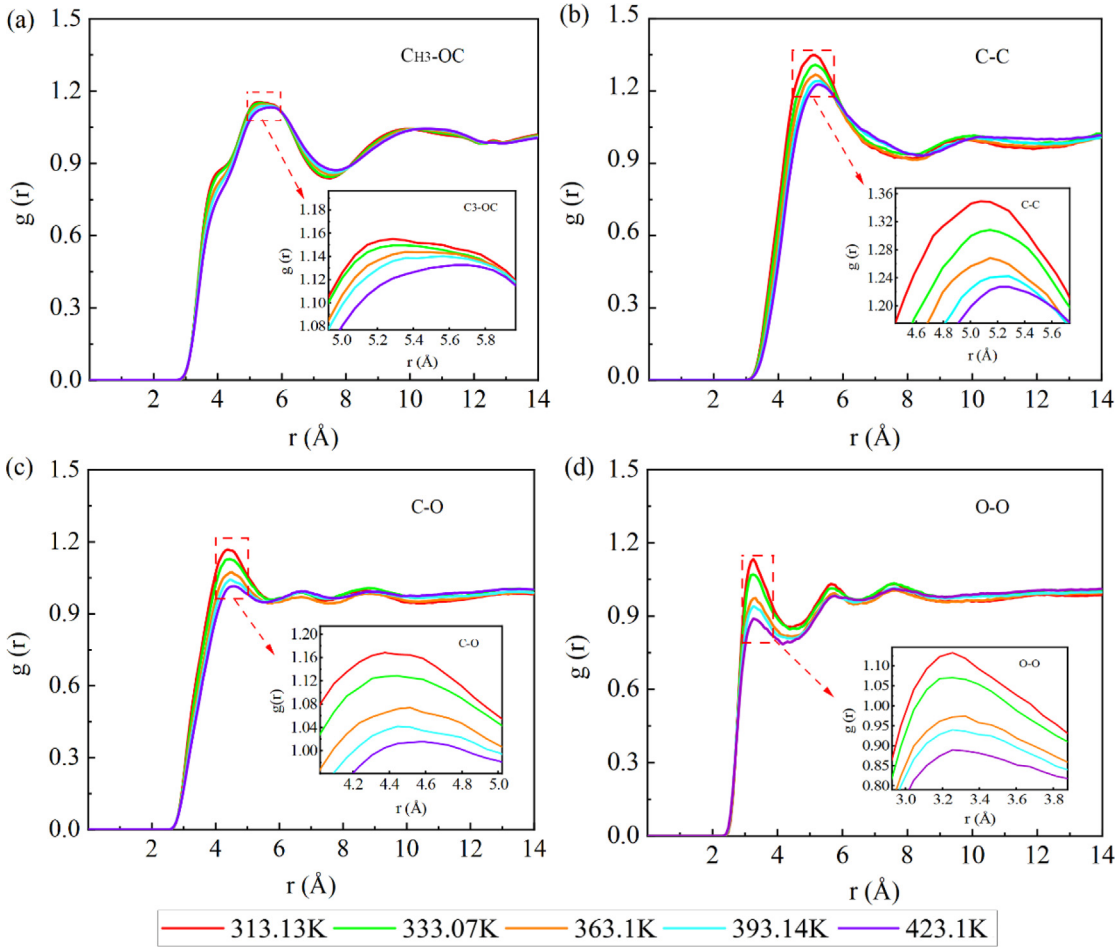

Fig. 9. RDFs of the n-decane/ethyl decanoate mixture: (a) C_{H3}-OC; (b) C–C; (c) C-O; and (d) O-O.

cosities of esters. Based on the above-mentioned simulations, we recommend the PCFF FF for ethyl decanoate and their mixtures with n-decane when predicting the viscosity and density.

3.2. Viscosity and density of ethyl dodecanoate and its mixture with n-decane

The PCFF FF is employed in subsequent simulations of ethyl dodecanoate and its mixture with the alkane component n-decane. Both kinematic viscosity and density of pure ethyl dodecanoate are calculated via MD simulations at temperatures from 302.83 K to 353.58 K under 0.1 MPa comparable with the experimental data [11], as shown in Fig. 5. It indicates that the simulation results of viscosity and density of pure ethyl dodecanoate by the PCFF FF are well comparable with the experimental data. In addition, the AAREs for viscosity and density are only 7.43% and 0.64%, respectively.

The calculated viscosities and densities of a binary mixture of n-decane and ethyl dodecanoate by the PCFF FF are shown in Fig. 6. Both simulated values of viscosity and density are in good agreement with the experimental data [37] with the AAREs of 5.62% for viscosity and 0.205% for density at temperatures from 313.13 K to 422.96 K under pressures from 0.11 MPa to 0.18 MPa. Since the limitation of experimental data of pure ethyl dodecanoate, viscosities of binary mixture of ethyl dodecanoate and n-decane by the UV model are obtained at temperatures from 313.13 K to 348.05 K with an AARE of 4.19%.

Here the UV model has a slightly better accuracy than the PCFF FF. However, as shown in Section 3.1, the prediction accuracy of the UV model is much worse than the PCFF FF for the mixture of ethyl decanoate and n-decane. Considering the overall prediction accuracy for the binary mixtures of n-decane with ethyl decanoate and n-decane with ethyl dodecanoate, the PCFF FF outperforms the UV model in the predictions.

3.3. Self-diffusion coefficient

The time-dependent mean square displacement (MSD) is used to calculate the self-diffusion coefficient in MD simulations, and it requires a finite-size correction (Yeh-Hummer correction) [40]. To fit the self-diffusion coefficient, we need to find a time range. Here an effective time range is determined in a region with a slope in log (MSD)-log (t) curve that is closed to 1[41].

The MSDs of pure n-decane, ethyl decanoate and their mixtures are calculated, as shown in Fig. 7(a)-(c). The MSDs exhibit a linear relationship with the simulation time and the slope of MSDs increases with the increasing of temperature. The self-diffusion coefficients of pure n-decane, ethyl decanoate with or without Yeh-Hummer correction are depicted in Fig. 7(d) as a function of temperature. It indicates that the self-diffusion coefficients for both n-decane and ethyl decanoate rise non-linearly when the temperature increases, indicating that the molecules' diffusion ability is strengthened with the temperature rising. In general, self-diffusion coefficients and viscosity of the molecular liquids follow the opposite trend. The liquid viscosity is derived from the

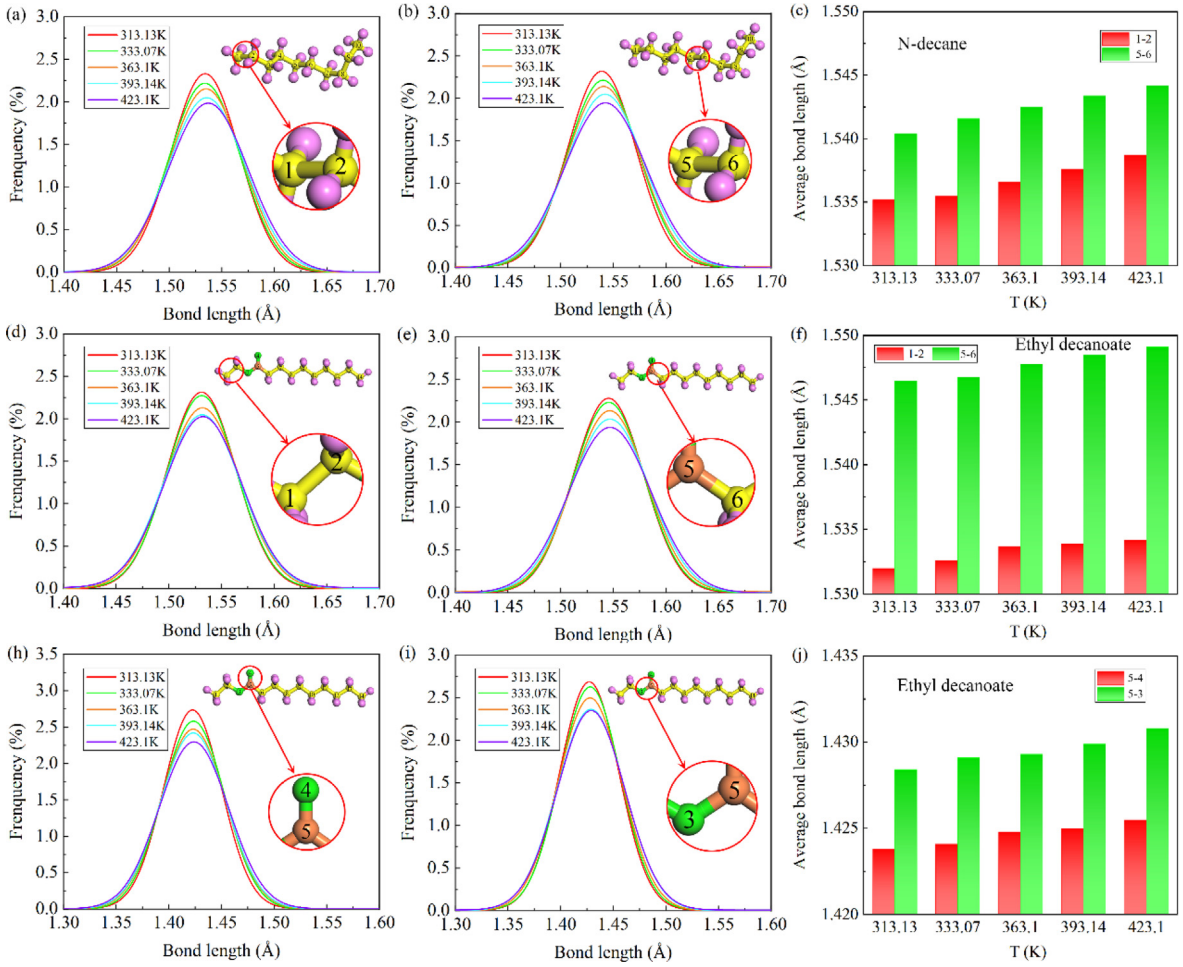

Fig. 10. Bond length distribution function of n-decane and ethyl decanoate in the mixture and the average bond length: (a)-(c) N-decane; (d)-(j) Ethyl decanoate.

internal friction and intermolecular attraction between different molecules. Moreover, as the temperature increases, the intermolecular distance of the molecules of n-decane or ethyl decanoate gets larger due to the volume expansion, which lowers the intermolecular attraction and further results in a decreasing viscosity.

3.4. Microscopic analysis

The atom number of the molecular chains of n-decane and ethyl decanoate involved in the following microscopic analysis is shown in Fig. 8.

3.4.1. Radial distribution function

The radial distribution function (RDF), also called g(r), represents how the liquid density varies as a function of the distance away from a reference particle [42]. Fig. 9 illustrates the RDFs of the binary mixture of n-decane and ethyl decanoate at different temperatures. The atom types are corresponding to those in Table 1. The RDFs decay near 1 within its truncation radius. Fig. 9(a) sees the first peaks of $g(r)_{C_{H_3}\text{-}OC}$ located at about 5.27 Å for T = 313.13 K and 5.75 Å for T = 423.1 K. In addition, the right shifts of the peak show that the distance between n-decane molecules and ethyl decanoate molecules gradually rises with the increasing of temperature. Fig. 9(b), (c) and (d) illustrate the first peak positions of $g(r)_{C\text{-}C}$, $g(r)_{C\text{-}O}$ and $g(r)_{O\text{-}O}$ shift to the right steadily as the temperature increases from 313.13 K to 423.1 K, which indicates the distance between ethyl decanoate molecules gradually increases with the increasing of temperature. Moreover, the magnitudes of the major peaks of $g(r)_{C_{H_3}\text{-}OC}$, $g(r)_{C\text{-}C}$, $g(r)_{C\text{-}O}$ and $g(r)_{O\text{-}O}$ decrease as the temperature rises. It means that as the temperature increases, the degree of aggregation of the n-decane and ethyl decanoate molecules reduces, as does the degree of aggregation between n-decane and ethyl decanoate molecules, leading to a reduced density of the mixture.

3.4.2. Bond length

We statistically collect the bond lengths of n-decane and ethyl decanoate in their mixture at different temperatures. For n-decane, the chain head bond 1–2 and the chain bond 5–6 are chosen; while for ethyl decanoate, the chain head bond 1–2 and the chain bonds 5–6, 4–5, 3–5 are chosen. The bond lengths of bond 1–2 and bond 5–6 of n-decane mainly range from 1.450 Å to 1.650 Å and show an almost uniform distribution, as illustrated in Fig. 10(a) and (b). As the temperature rises, the peak of the bond length distribution function shifts to the right and drops, indicating

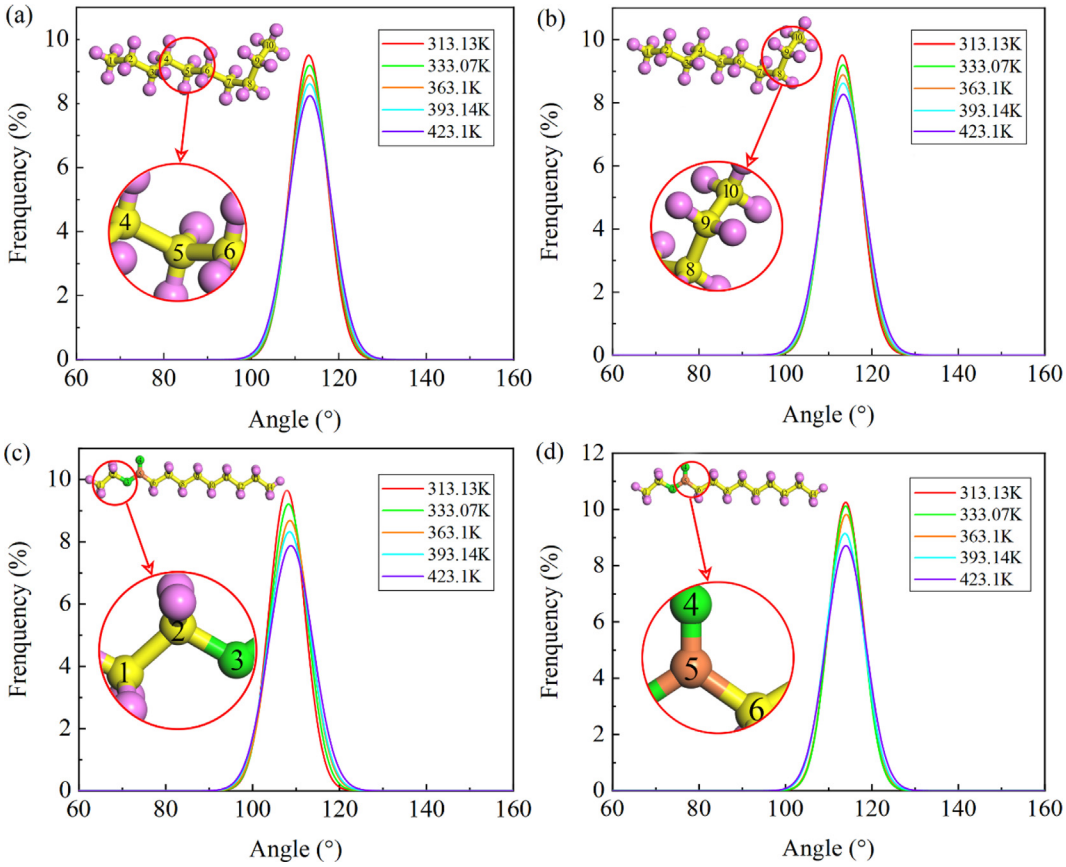

Fig. 11. Angular distribution function of n-decane and ethyl decanoate in their mixture: (a) and (b) N-decane; (c) and (d) Ethyl decanoate.

that the average bond length increases with the temperature. The bond length distribution functions of bond 1–2 and bond 5–6 of ethyl decanoate are dispersed between 1.450 Å and 1.650 Å, as shown in Fig. 10(d) and (e). The bond length distribution functions of ethyl decanoate bonds 4–5 and 3–5 are both distributed ranging from 1.325 Å to 1.525 Å, as can be seen in Fig. 10(h) and (i). The variation trend of bond length distribution function of ethyl decanoate with temperature is consistent with that of n-decane, and the bond length of ethyl decanoate increases with the increasing of temperature, as shown in Fig. 10(f) and (j).

3.4.3. Angular distribution function

A three-body correlation function is constructed by using the coordinates of atoms recorded during the computation process and is used to describe the angular distribution function (ADF). The nearest atom for a center atom is first determined using the associated atom RDF graph. A central atom i is then used as the vertex, while another two arbitrarily closest atoms j and k are used as the end points, and the angles of the three atoms are calculated using the formula [19]:

$$\theta_{jik} = \left\langle \cos^{-1}\left(\frac{r_{ij}^2 + r_{ik}^2 - r_{jk}^2}{2r_{ij}r_{ik}}\right) \right\rangle \tag{15}$$

The ADFs of the mixture of n-decane and ethyl decanoate are used to analyze the changes of bond angles under pressures from 0.11 MPa to 0.18 MPa at temperatures from 313.13 K to 423.1 K, which is shown in Fig. 11. For n-decane, the bond angles 4–5–6 in the chain and 8–9-10 at the chain tail are selected; while for ethyl decanoate, the bond angles 1–2–3 at the chain head and 4–5–6 in the chain are chosen. In Fig. 11(a) and (b), the peaks of the angles of 4–5–6 and 8–9–10 of the n-decane molecule concentrated near their initial value of 114° decrease and their distribution regions broaden with the increasing of temperature. Fig. 11 (c) and (d) see the similar tendencies in ADFs of ethyl decanoate molecules with angles 1–2–3 and 4–5–6, and the values of peaks are reduced and the changing range of the angles 1–2–3 and 4–5–6 becomes wider with the increasing of temperature. These results show that when the temperature rises, the angle variation between neighboring bonds develops but the average bond angle almost doesn't change.

3.4.4. End-to-end length

The results of end-to-end lengths of n-decane and ethyl decanoate molecules in their mixture at various temperatures and pressures are shown in Fig. 12. The distribution functions of end-to-end lengths are depicted in Fig. 12(a)-(b), in which the end-to-end lengths of n-decane and ethyl decanoate are primarily dispersed in the ranges of 8–12 Å and 10–16 Å, respectively. The peaks of the distribution function for end-to-end length swing to the left and subsequently drop as the temperature rises, indicating the decreased end-to-end lengths of n-decane and ethyl decanoate. In addition, we calculate the averaged end-to-end length of n-decane and ethyl decanoate, as shown in Fig. 12(c) and (d). It can be clearly seen that as the temperature goes up the end-to-end length of n-decane and ethyl decanoate is decreasing. However,

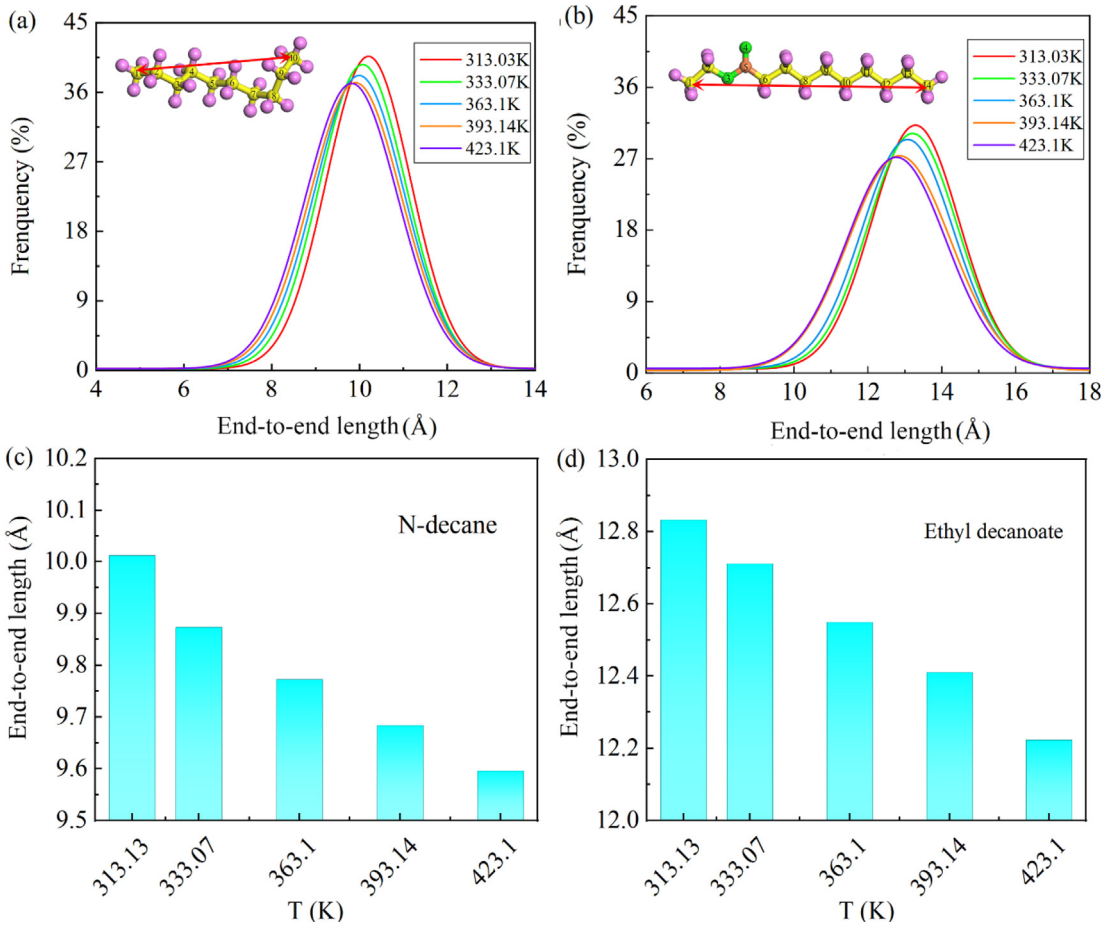

Fig. 12. End-to-end length of n-decane and ethyl decanoate in their mixture: (a) and (c) N-decane; (b) and (d) Ethyl decanoate.

such decreased end-to-end lengths are not resulted from the change of the bond length and bond angle, because we have found that the bond length increases with the temperature while the average bond angle almost doesn't change. This suggests that the molecular chains become more twisted and shrunk with the increasing of temperature. Furthermore, as the end-to-end length of molecular chains decreases, the radius of gyration decreases too, which results in the reduction of viscosity.

3.4.5. Dihedral distribution

The dihedral angle analysis of n-decane and ethyl decanoate in their mixture is shown in Fig. 13. For n-decane, the atomic group 7, 8, 9, 10 at the chain tail and atomic group 3, 4, 5, 6 in the chain are selected; while for ethyl decanoate, atomic group 1, 2, 3, 5 at the chain head, as well as atomic group 4, 5, 6, 7 in the chain are chosen. Fig. 13(a) and (b) show the dihedral angle distributions of n-decane. Particularly, the observed distribution has three peaks: two small peaks around 60° and 300° directly correlate to two gauche conformations, and the highest peak around 180° corresponds to a dihedral angle in the *trans*-conformation relating to the global energy minimum [43]. It can be seen that the highest peak of dihedral angle distribution function at 180° decreases with the increasing of temperature, which means that the twist of the chains becomes more noticeable. Fig. 13(c) and (d) depict the dihedral angle distribution of ethyl decanoate, which is consistent with n-decane for variation trend of highest peak, but inconsistent for the two minor peaks. It is worth noting that the distribution curve of the dihedral angle contains no minor peak for group 4, 5, 6, 7, which may be related to the carbonyl group, and the two minor peaks locate at near 80° and 280° for group 1, 2, 3, 5, respectively. Since a slight increase in bond length is reported in simulations, we conclude that the deceasing end-to-end lengths of the n-decane molecules is due to the chain twist. In addition, the degree of distortion of the n-decane and ethyl decanoate molecular chains increases as temperature going up, which explains why their end-to-end lengths decrease as the temperature rises.

Thus, based on the above-mentioned microscopic analysis, it can be concluded that the distance between molecules in the mixtures increases with the increasing of temperature, but the end-to-end lengths of molecule chains decrease as the temperature rises. The former will lead to a reduced density. The latter is resulted from the chain twist and shrinking due to the variation of dihedral of the molecules rather than the variation of the bond length and bond angles of molecules. The decreased end-to-end lengths with the increasing of temperature lead to a decreasing radius of gyration (R_g) of molecule chains, which also contributes to the decrease of viscosity considering viscosity $\eta \propto R_g^2$ in the Rouse model [44].

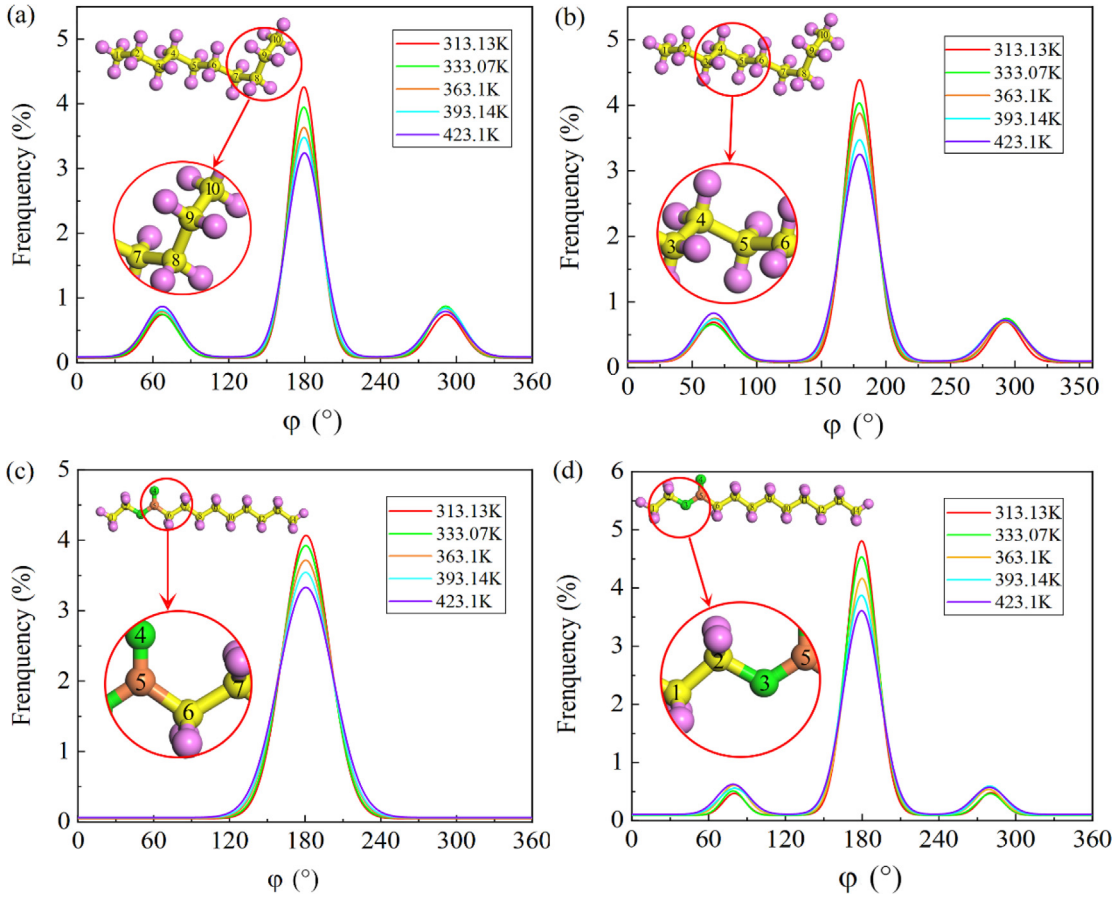

Fig. 13. Dihedral angle distributions of n-decane and ethyl decanoate in their mixture at different temperatures: (a) and (b) N-decane; (c) and (d) Ethyl decanoate.

4. Conclusion

In summary, the thermophysical properties such as the kinematic viscosity and density, and the structure of fuel blends containing n-decane and biofuel compound of ethyl decanoate and ethyl dodecanoate have been investigated by MD method. The COMPASS FF and the PCFF FF are adopted and compared in the simulation, and the calculated viscosities by using both FFs are compared with those by UV model. MD simulation results with the PCFF FF show better prediction accuracy for both viscosity and density than the COMPASS FF. For mixture of n-decane and ethyl decanoate, the AAREs of 7.08% and 0.32 % by using the PCFF FF are reported for viscosity and density, and the corresponding AAREs are 5.62 % and 0.205 % for mixture of n-decane and ethyl dodecanoate. The UV model is employed to calculate the viscosities of mixtures, having AARE of 12.22% for mixture of n-decane and ethyl decanoate and 4.19% for mixture of n-decane and ethyl dodecanoate. In addition, the self-diffusion coefficient, the radial distribution function, the bond length distribution function, the angular distribution function, the end-to-end length distribution function, and the dihedral angle distribution function of the mixture of n-decane and ethyl decanoate are analyzed. It is found that the bond length of n-decane and ethyl decanoate molecules increases with the increasing of temperature but the corresponding end-to-end length decreases. This demonstrates that the twist and shrink of molecular chains become intense with the increasing of temperature. The shrink of molecular chain combined with the growing intermolecular distance leads to a noticeable decrease in the mixture's kinematic viscosity.

So far, numerical studies on the thermophysical properties of bio-aviation fuel containing fatty acid esters are still limited. The present work in this study provides a baseline for simulations to predict the thermophysical properties (i.e., viscosity and density) of fuel blends consisting of n-alkanes and fatty acid esters, thus can help the further investigations of bio-aviation kerosene and optimize the design of the regenerative cooling systems and the engine injection systems of the aero-engines [37].

CRediT authorship contribution statement

Xueming Yang: Conceptualization, Methodology, Validation, Writing – original draft. **Qiang Liu:** Investigation, Formal analysis, Writing – review & editing. **Yongfu Ma:** Visualization, Validation. **Jianfei Xie:** Writing – review & editing, Validation. **Bingyang Cao:** Supervision, Software.

Data availability

I have shared the link to my data at the Attach File step

Declaration of Competing Interest

The authors declare that they have no known competing financial interests or personal relationships that could have appeared to influence the work reported in this paper.

Acknowledgments

This research is supported by the National Science and Technology Major Project of China (Grant No. 2017-III-0005-0030) and the Natural Science Foundation of Hebei Province of China (Grant No. E2019502138). This work was carried out at Shanxi Supercomputing Center of China, and the simulations were performed upon TianHe-2.

Appendix A. Supplementary material

Supplementary data to this article can be found online at https://doi.org/10.1016/j.molliq.2023.121680.

References

[1] P. Maciejczyk, L.-C. Chen, G. Thurston, The role of fossil fuel combustion metals in PM2. 5 air pollution health associations, Atmosphere 12 (2021) 1086, doi: 10.3390/atmos12091086.
[2] F. Perera, K. Nadeau, Climate change, fossil-fuel pollution, and children's health, N. Engl. J. Med. 386 (2022) 2303, https://doi.org/10.1056/NEJMra2117706.
[3] J.S. Kinsey, M.T. Timko, S.C. Herndon, E.C. Wood, Z. Yu, R.C. Miake-Lye, P. Lobo, P. Whitefield, D. Hagen, C. Wey, B.E. Anderson, A.J. Beyersdorf, C.H. Hudgins, K. L. Thornhill, E. Winstead, R. Howard, D.I. Bulzan, K.B. Tacina, W.B. Knighton, Determination of the emissions from an aircraft auxiliary power unit (APU) during the Alternative Aviation Fuel Experiment (AAFEX), J Air Waste Manag Assoc. 62 (2012) 420, https://doi.org/10.1080/10473289.2012.655884.
[4] Y. Shen, Y. Liu, B. Cao, C4+ surrogate models for thermophysical properties of aviation kerosene RP-3 at supercritical pressures, Energy Fuel 35 (2021) 7858, https://doi.org/10.1021/acs.energyfuels.1c00326.
[5] B. Yu, X. Jiang, D. He, C. Wang, Z. Wang, Y. Cai, J. Yu, J.J. Yu, Development of a chemical-kinetic mechanism of a four-component surrogate fuel for RP-3 kerosene, ACS Omega 6 (2021) 23485, https://doi.org/10.1021/acsomega.1c03442.
[6] B.-Y. Wang, Y.-X. Liu, J.-J. Weng, G.-F. Pan, Z.-Y. Tian, An experimental and modeling study on the low temperature oxidation of surrogate for JP-8 part II: Comparison between neat 1, 3, 5-trimethylbenzene and its mixture with n-decane, Combust Flame 192 (2018) 517, https://doi.org/10.1016/j.combustflame.2018.01.001.
[7] L. Zhao, T. Yang, R.I. Kaiser, T.P. Troy, M. Ahmed, D. Belisario-Lara, J.M. Ribeiro, A.M. Mebel, Combined experimental and computational study on the unimolecular decomposition of JP-8 jet fuel surrogates. I. n-Decane (n-C10H22), J. Phys. Chem. A. 121 (2017) 1261, doi: 10.1021/acs.jpca.6b11472.
[8] J. Liu, E. Hu, W. Zeng, W. Zheng, A new surrogate fuel for emulating the physical and chemical properties of RP-3 kerosene, Fuel 259 (2020), https://doi.org/10.1016/j.fuel.2019.116210.
[9] W. Liu, X. Liang, B. Lin, H. Lin, Z. Huang, D. Han, A comparative study on soot particle size distributions in premixed flames of RP-3 jet fuel and its surrogates, Fuel 259 (2020), https://doi.org/10.1016/j.fuel.2019.116222.
[10] Y. Zhang, T. Zhan, J. Chen, X. Liu, M. He, Experimental investigation and modeling of thermophysical properties of ethyl decanoate at high temperatures, Fluid Phase Equilib. 501 (2019), https://doi.org/10.1016/j.fluid.2019.112274.
[11] M. He, T. Lai, X. Liu, Measurement and correlation of viscosities and densities of methyl dodecanoate and ethyl dodecanoate at elevated pressures, Thermochim. Acta 663 (2018) 85, https://doi.org/10.1016/j.tca.2018.03.007.
[12] G. Zhao, X. Liu, Z. Yuan, J. Yin, S. Ma, Liquid surface tension, kinematic viscosity, density and refractive index of the binary mixtures of n-hexadecane with methyl butyrate and methyl decanoate close to saturation conditions, Fluid Phase Equilib. 510 (2020), https://doi.org/10.1016/j.fluid.2019.112448.
[13] A. Alkhwaji, S. Elbahloul, M.Z. Abdullah, K.F.B.A. Bakar, Selected water thermal properties from molecular dynamics for engineering purposes, J. Mol. Liq. 324 (2021), https://doi.org/10.1016/j.molliq.2020.114703.
[14] X. Zhao, T. Luo, H. Jin, A predictive model for self-, Maxwell-Stefan, and Fick diffusion coefficients of binary supercritical water mixtures, J. Mol. Liq. 324 (2021), https://doi.org/10.1016/j.molliq.2020.114735.
[15] Y. Zhou, Y. Li, Molecular dynamics simulation of kinetic boundary conditions and evaporation/condensation coefficients of direct-contact condensation in two-phase jet, AIP Adv. 12 (2022), https://doi.org/10.1063/5.0092010.
[16] J. Nichele, A.B. de Oliveira, L.S.d.B. Alves, I. Borges, Accurate calculation of near-critical heat capacities C P and C V of argon using molecular dynamics, J. Mol. Liq. 237 (2017) 65, doi: 10.1016/j.molliq.2017.03.120.
[17] Y. Wang, S. Gong, L. Li, G. Liu, Sub-to-supercritical properties and inhomogeneity of JP-10 using molecular dynamics simulation, Fuel 288 (2021), https://doi.org/10.1016/j.fuel.2020.119696.
[18] X. Yang, Q. Liu, X. Zhang, C. Ji, B. Cao, A molecular dynamics simulation study of the densities and viscosities of 1,2,4-trimethylbenzene and its binary mixture with n-decane, Fluid Phase Equilib. 562 (2022), https://doi.org/10.1016/j.fluid.2022.113566.
[19] X. Yang, J. Tao, Q. Liu, X. Zhang, B. Cao, Molecular dynamics simulation of thermophysical properties of binary RP-3 surrogate fuel mixtures containing trimethylbenzene, n-decane, and n-dodecane, J. Mol. Liq. (2022) 119258, doi: 10.1016/j.molliq.2022.119258.
[20] S. Maskey, B.H. Morrow, M.Z. Gustafson, D.J.L. Prak, P.T. Mikulski, J.A. Harrison, Systematic examination of the links between composition and physical properties in surrogate fuel mixtures using molecular dynamics, Fuel 261 (2020) 116247, doi: 10.1016/j.fuel.2019.116247.
[21] D.J. Luning Prak, B.H. Morrow, J.S. Cowart, P.C. Trulove, J.A. Harrison, Thermophysical properties of binary mixtures of n-dodecane with n-alkylcyclohexanes: experimental measurements and molecular dynamics simulations, J. Chem. Eng. Data. 64 (2019) 1550, doi: 10.1021/acs.jced.8b01135.
[22] M.L. Huber, NIST Thermophysical properties of hydrocarbon mixtures database (SUPERTRAPP), version 3.2, (2007).
[23] Z. Yuan, X. Zhang, Y. Wang, W. Nie, J. Yin, S. Ma, G. Zhao, Thermophysical properties of the binary mixtures of iso-octane with methyl hexanoate, n-decane with methyl decanoate and methyl octanoate: experimental investigation and molecular dynamic simulation, Fluid Phase Equilib. 544–545 (2021), https://doi.org/10.1016/j.fluid.2021.113099.
[24] W. Zhu, X. Wang, J. Xiao, W. Zhu, H. Sun, H. Xiao, Molecular dynamics simulations of AP/HMX composite with a modified force field, J. Hazard. Mater. 167 (2009) 810, https://doi.org/10.1016/j.jhazmat.2009.01.052.
[25] H. Sun, COMPASS: an ab initio force-field optimized for condensed-phase applications overview with details on alkane and benzene compounds, J. Phys. Chem. B. 102 (1998) 7338, https://doi.org/10.1021/jp980939v.
[26] H. Sun, Force field for computation of conformational energies, structures, and vibrational frequencies of aromatic polyesters, J. Comput. Chem. 15 (1994) 752, https://doi.org/10.1002/jcc.540150708.
[27] J. Blomqvist, L. Ahjopalo, B. Mannfors, L.-O. Pietilä, Studies on aliphatic polyesters I: Ab initio, density functional and force field studies of esters with one carboxyl group, J. Mol. Struct. (Thoechem) 488 (1999) 247, https://doi.org/10.1016/S0166-1280(99)00038-X.
[28] D. Boda, D. Henderson, The effects of deviations from Lorentz-Berthelot rules on the properties of a simple mixture, Mol. Phys. 106 (2008) 2367, https://doi.org/10.1080/00268970802471137.
[29] S. Hajilar, B. Shafei, Thermal transport properties at interface of fatty acid esters enhanced with carbon-based nanoadditives, INT J. HEAT MASS TRAN. 145 (2019), https://doi.org/10.1016/j.ijheatmasstransfer.2019.118762.
[30] S. Hajilar, B. Shafei, Multiscale investigation of interfacial thermal properties of n-octadecane enhanced with multilayer graphene, J. Phys. Chem. C. 123 (2019) 23297, https://doi.org/10.1021/acs.jpcc.9b03042.
[31] S. Pricl, M. Fermeglia, Virtual rheological experiments on linear alkane chains confined between titanium walls, Rheol. Acta 40 (2001) 104, https://doi.org/10.1007/s003970000148.
[32] N.D. Kondratyuk, V.V. Pisarev, Calculation of viscosities of branched alkanes from 0.1 to 1000 MPa by molecular dynamics methods using COMPASS force field, Fluid Phase Equilib. 498 (2019) 151, doi: 10.1016/j.fluid.2019.06.023.
[33] S. Plimpton, Fast parallel algorithms for short-range molecular dynamics, J. Comput. Phys. 117 (1995) 1, https://doi.org/10.1006/jcph.1995.1039.
[34] C. Chen, X. Jiang, Y. Sui, Prediction of transport properties of fuels in supercritical conditions by molecular dynamics simulation, Energy Procedia 158 (2019) 1700, https://doi.org/10.1016/j.egypro.2019.01.396.
[35] X. Yang, Y. Gao, M. Zhang, W. Jiang, B. Cao, Comparison of atomic simulation methods for computing thermal conductivity of n-decane at sub/supercritical pressure, J. Mol. Liq. 342 (2021), https://doi.org/10.1016/j.molliq.2021.117478.
[36] G. Zhao, Z. Yuan, J. Yin, S. Ma, Thermophysical properties of fatty acid methyl and ethyl esters, J. Chem. Thermodyn. 134 (2019) 195, https://doi.org/10.1016/j.jct.2019.02.025.
[37] Z. Yuan, G. Zhao, X. Zhang, J. Yin, S. Ma, Experimental investigation and correlations of thermophysical properties for bio-aviation kerosene surrogate containing n-decane with ethyl decanoate and ethyl dodecanoate, J. Chem. Thermodyn. 150 (2020), https://doi.org/10.1016/j.jct.2020.106201.
[38] Y. Gaston-Bonhomme, P. Petrino, J.L. Chevalier, UNIFAC—VISCO group contribution method for predicting kinematic viscosity: extension and temperature dependence, Chem. Eng. Sci. 49 (1994) 1799, https://doi.org/10.1016/0009-2509(94)80065-0.
[39] D.M. Bajić, E.M. Živković, S.P. Šerbanović, M.L. Kijevčanin, Experimental measurements and modelling of volumetric properties, refractive index and viscosity of selected binary systems with butyl lactate at 288.15–323.15 K and atmospheric pressure. New UNIFAC-VISCO interaction parameters, Thermochim. Acta 562 (2013) 42, doi: 10.1016/j.tca.2013.03.025.
[40] I.-C. Yeh, G. Hummer, System-size dependence of diffusion coefficients and viscosities from molecular dynamics simulations with periodic boundary conditions, J. Phys. Chem. B. 108 (2004) 15873, doi: 10.1021/jp0477147.
[41] X. Wang, L. Sun, X. Zhang, S. Zhang, J. Wang, Y. Zhang, The effect of nanoparticles on the microstructure of alkanes: a molecular dynamics study, J. Mol. Liq. 309 (2020), https://doi.org/10.1016/j.molliq.2020.113162.
[42] X. Yang, M. Zhang, Y. Gao, J. Cui, B. Cao, Molecular dynamics study on viscosities of sub/supercritical n-decane, n-undecane and n-dodecane, J. Mol. Liq. 335 (2021), https://doi.org/10.1016/j.molliq.2021.116180.
[43] D.A. Bernard-Brunel, J.J. Potoff, Effect of torsional potential on the predicted phase behavior of n-alkanes, Fluid Phase Equilib. 279 (2009) 100, https://doi.org/10.1016/j.fluid.2009.02.008.
[44] M. Mondello, G.S. Grest, E.B. Webb III, P. Peczak, Dynamics of n-alkanes: comparison to Rouse model, J. Chem. Phys. 109 (1998) 798, https://doi.org/10.1063/1.476619.